Supplemental Information

Osteogenic Differentiation in Bone Marrow Mesenchymal Stromal Cells Confers a Proliferative Advantage to Resident Leukemia Cells

V. Lokesh Battula[1*], Phuong M. Le[1], Jeffrey C. Sun[1], Khoa Nguyen[1], Bin Yuan[1], Ximin Zhou[1], Sonali Sonnylal[1], Teresa McQueen[1], Vivian Ruvolo[1], Keith A. Michel[2], Xiaoyang Ling[1], Rodrigo Jacamo[1], Elizabeth Shpall[3], Zhigiang Wang[4], Arvind R Uppore Kukkillaya[5], Gheath Al-Altrash[3], Marina Konopleva[1], R. Eric Davis[4], Melvyn A. Harrington[6], Catherine W. Palisch[6], Carlos Bueso-Ramos[7], Michael Andreeff[1,2*]

[1]Molecular Hematology and Therapy, Department of Leukemia, [2]Small Animal Imaging Facility (SAIF), [3]Department of Stem Cell Transplantation and Cellular Therapy, [4]Department of Lymphoma and Myeloma, [5]Department of Bioinformatics and Computational Biology, University of Texas MD Anderson Cancer Center, Houston, TX. [6]Orthopedic Surgery, Baylor College of Medicine, Houston, TX. [7]Department of Hematopathology, University of Texas MD Anderson Cancer Center, Houston, TX.

	TNAP MFI	Age	Disease status	Gender	Blast%	WBC K/µl	Type of AML (WHO)
1	14222	58	Relapsed	Female	71%	6.8	Therapy related-M2
2	836	67	Remission	Male	1%	0.7	AML with myelodysplasia
3	526	63	Remission	Male	1%	1.7	AML
4	3277	55	Relapsed	Male	20%	0.8	AML
5	7018	53	Relapsed	Male	91%	44.5	AML with Multi-lineage displacia-M4
6	6982	60	Remission	Female	32%	50	AML with Myelomonocytic Differentiation
7	2740	25	Relapsed	Female	72%	63.4	AML
8	511.6	69	Relapsed	Male	66%	58.5	Relapsed-refractory AML
9	952	47	Relapsed	Male	55%	12.5	AML with minimal differentiation
10	360	46	Relapsed	Male	65%	1.1	AML with maturation-M2
11	16927	33	Relapsed	Male	49%	17.4	AML with maturation-M2
12	672	44	Remission	Male	86%	55.1	AML with Inv(16)
13	13359	58	Relapsed	Female	40%	3.2	AML with maturation-M2
14	1068.1	56	Remission	Female	6%	0.1	Therapy related-M2
15	576.9	43	Relapsed	Female	88%	21.3	Therapy related-M2
16	3914	59	Relapsed	Female	83%	9.4	AML with myelodysplasia
17	998	46	Remission	Male	12%	1.8	AML with maturation-M2
18	7608	62	New	Male	52%	39.4	AML with myelodysplasia
19	415.67	70	Relapsed	Male	59%	1.6	AML with myelodysplasia
20	17836	78	New	Male	77%	1.5	AML-M2
21	2675	63	New	Female	70%	11.3	AML-M0
22	16848	69	New	Male	32%	26.2	AML-M4-FAB
23	1508	55	New	Female	92%	92.3	Therapy related-M2
24	2186	68	New	Male	68%	15.9	AML
25	1784.5	61	Remission	Female	2%	3.8	AML-M4-FAB
26	451.5	62	Relapsed	Male	73%	0.7	AML with myelodysplasia
27	575.5	63	Relapsed	Male	67%	2	AML
28	1003	70	Relapsed	Male	22%	38.5	AML-FAB M5b
29	1786.5	70	Remission	Male	0%	3.6	AML-M0
30	176.1	63	Normal-BM	Female	NA	NA	Normal-BM-Donor
31	216.8	53	Normal-BM	Male	NA	NA	Normal-BM-Donor
32	147.8	62	Normal-BM	Female	NA	NA	Normal-BM-Donor
33	110.6	48	Normal-BM	Female	NA	NA	Normal-BM-Donor

34	369.9	50	Normal-BM	Male	NA	NA	Normal-BM-Donor
35	75.2	43	Normal-BM	Male	NA	NA	Normal-BM-Donor
36	144.4	60	Normal-BM	Male	NA	NA	Normal-BM-Donor
37	247.3	59	Normal-BM	Female	NA	NA	Normal-BM-Donor
38	62.8	58	Normal-BM	Femlae	NA	NA	Normal-BM-Donor
39	154	49	Normal-BM	Female	NA	NA	Normal-BM-Donor
40	83	57	Normal-BM	Female	NA	NA	Normal-BM-Donor

Supplementary Table 1. Characteristics of AML patient bone marrow donors. MSCs were isolated from BM samples from AML patients (sample 1-24) or normal donors (Samples 25-35) and subjected to flow cytometry for TNAP quantification. For each patient, TNAP mean fluorescence intensity (MFI), age, gender and percentage of blasts in the BM are listed. A gradient from blue to red was used to indicate the expression of TNAP in AML- and Normal-MSCs; dark blue being the lowest expresser and dark red being higher expresser. n/a signifies that information not available.

Function	Gene	Forward (5´-3´)	Reverse (5´-3´)
Osteoblast Differentiation	RUNX2	ATGTGTGTTTGTTTCAGCAGCA	TCCCTAAAGTCACTCGGTATGTGTA
	Osterix	TAGTGGTTTGGGGTTTGTTTTACC GC	AACCAACTCACTCTTATTCCCTAAGT
	Osteopontin (OPN)	TTGCAGCCTTCTCAGCCAA	GGAGGCAAAAGCAAATCACTG
	TNAP	CCTCCTCGGAAGACACTCTG	GCAGTGAAGGGCTTCTTGTC
Adipocyte Differentiation	aP2	AACCTTAGATGGGGGTGTCC	GTGGAAGTGACGCCTTTCAT
	PPAR-gamma	GCTGGCCTCCTTGATGAATA	TTGGGCTCCATAAAGTCACC
	Lipoprotein lipase	GGGCATGTTGACATTTACCC	GCTGGTCCACATCTCCAAGT
Others	CTGF	GCA GGC TAG AGA AGC AGAGC	TGG AGA TTT TGG GAG TAC GG
	Beta-actin	CTGGAACGGTGAAGGTGACG	AGTCCTCGGCCACATTGTGA
	GAPDH	GAGTCA ACG GAT TTG GTC GT	TTGATT TTG GAG GGA TCT CG

Supplementary Table 2. PCR primer sequences Sybr-green qRT-PCR. Primer sequences for genes involved in osteogenic and adipogenic genes and other genes involved in the study are listed.

Gene name	Taqman assay ID
BMP1	hs00241807_m1
BMP2	Hs00154192_m1
BMP4	Hs03676628_s1
BMP6	Hs01099594_m1
BMP7	Hs00233476_m1
BMP10	Hs00205566_m1
COL1A1	Hs00164004_m1
Bone Sialoprotein	Hs00173720_m1
Osteopontin	Hs00959010_m1
RUNX2	Hs01047973_m1
Osterix	Hs01866874_s1
Beta-2- microglobulin	Hs00187842_m1

Supplementary Table 3. List of Taqman gene expression assays used for qRT-PCR.

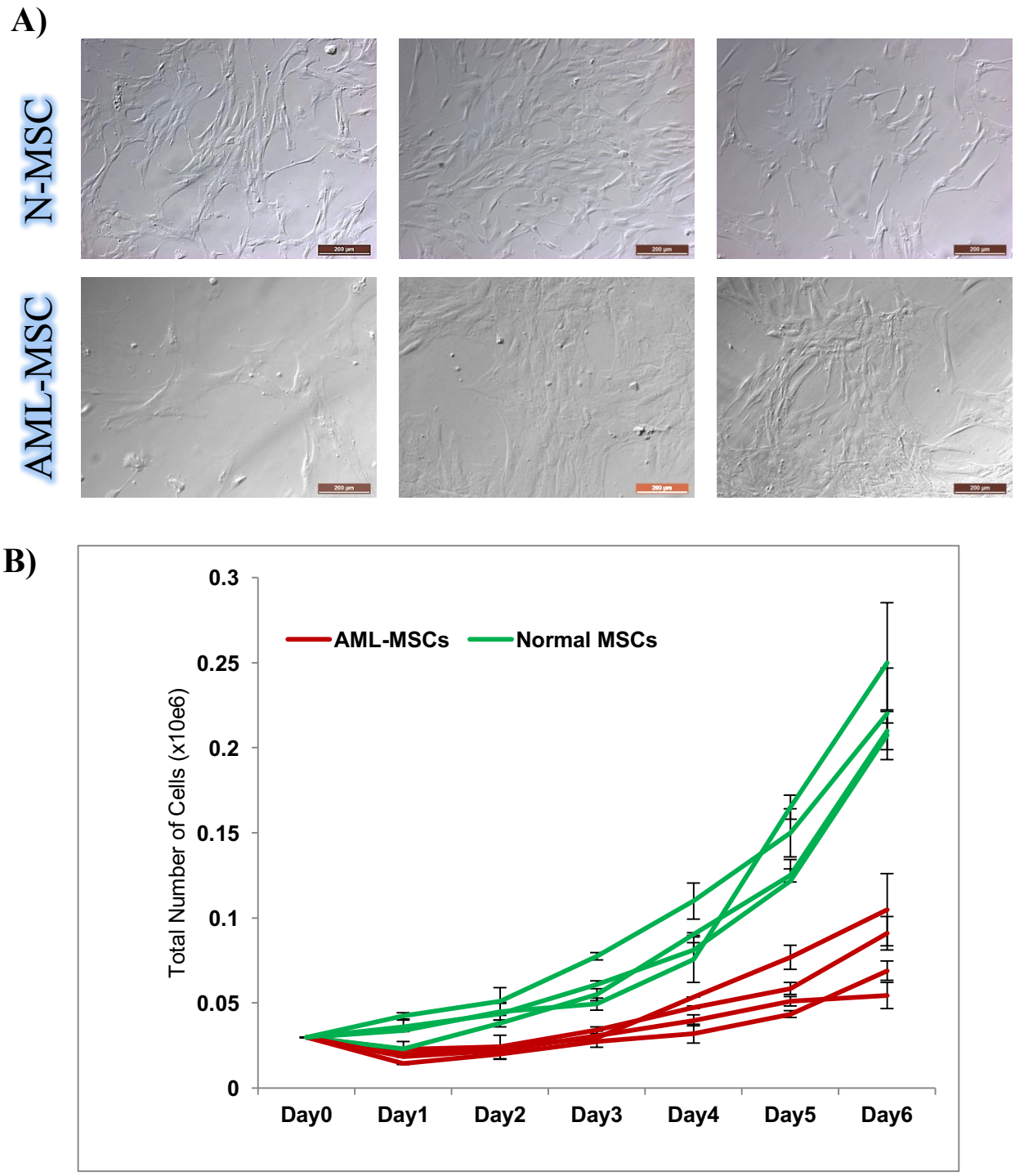

Supplementary Figure 1. *AML mesenchymal stem/stromal cells (MSCs) proliferate more slowly than normal MSCs (N-MSCs*). (a) Morphology of representative N-MSCs and AML-MSCs (n=4). Images were taken at passage 2-3. Scale bar, 200 µm. (b) Growth curves of N-MSCs and

AML-MSCs were obtained by counting absolute cell numbers with a trypan blue-based live cell counter daily for 7 days.

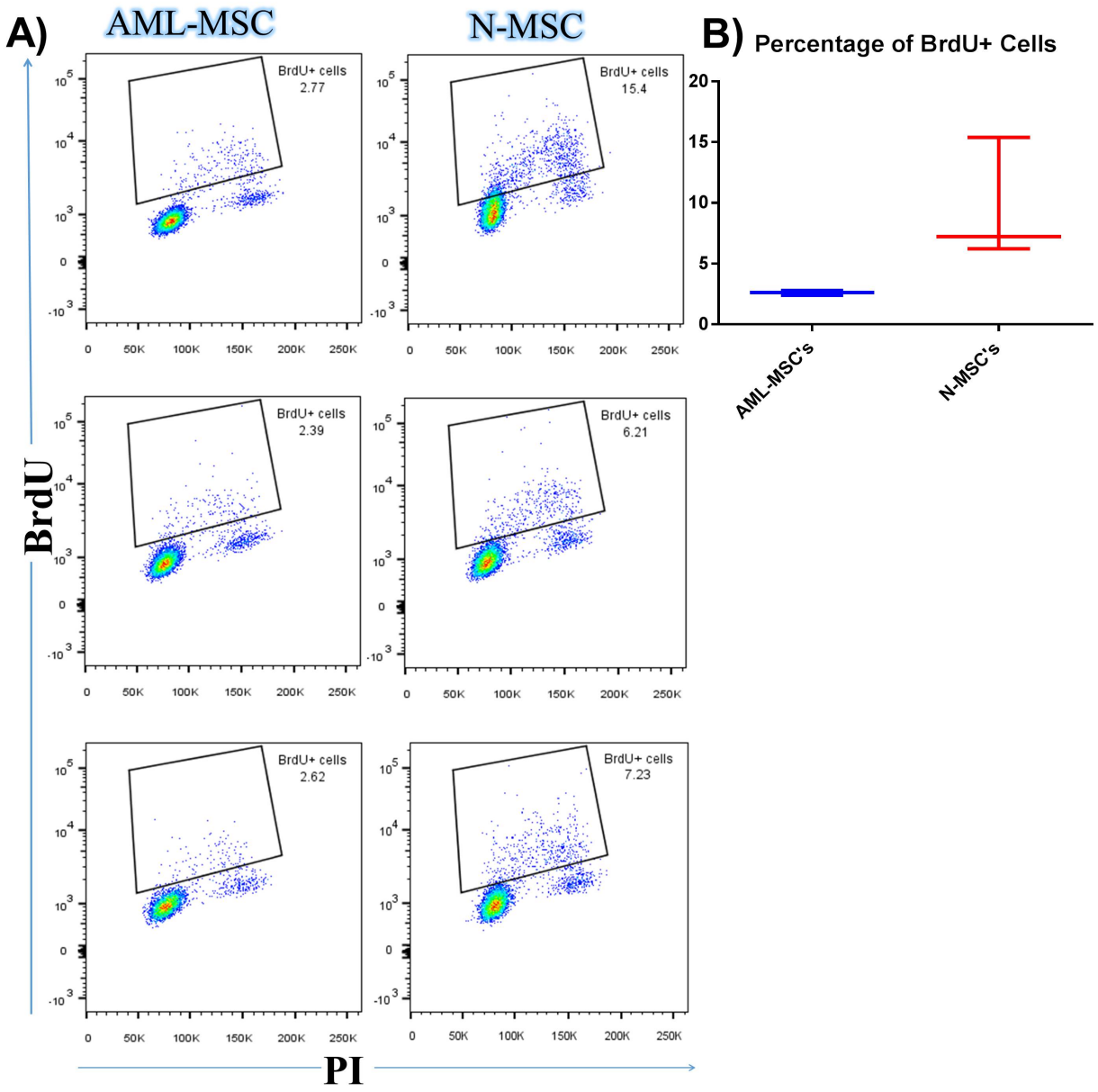

Supplementary Figure 2. *AML-MSCs proliferate more slowly than N-MSCs***.** Cell cycle progression of N-MSCs and AML-MSCs was analyzed by BrdU pulse/propidium iodide (PI) staining (n=5 per group). (a) Representative flow cytometric plots and (b) quantification of N- and AML-MSCs in S/G2 phase. Data were analyzed by FlowJo software (p<0.03).

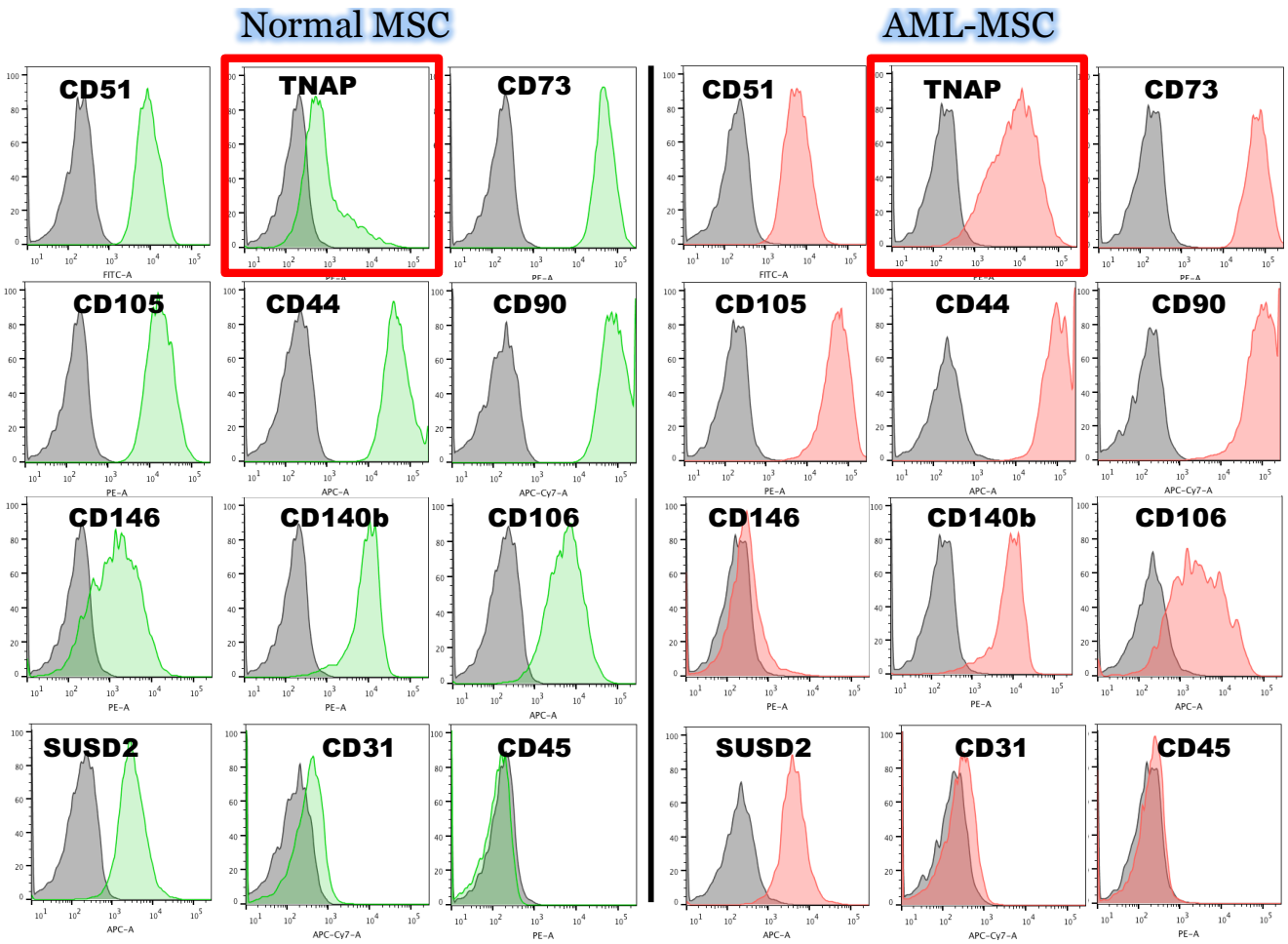

Supplementary Figure 3. *AML-MSCs express higher levels of tissue-nonspecific alkaline phosphatase (TNAP) Compared to Normal-MSCs* . N-MSCs and AML-MSCs were immunophenotyped for indicated cell surface markers by flow cytometry. Data were analyzed by FlowJo software. Differential expression of TNAP in N- and AML-MSCs is highlighted by the red boxes.

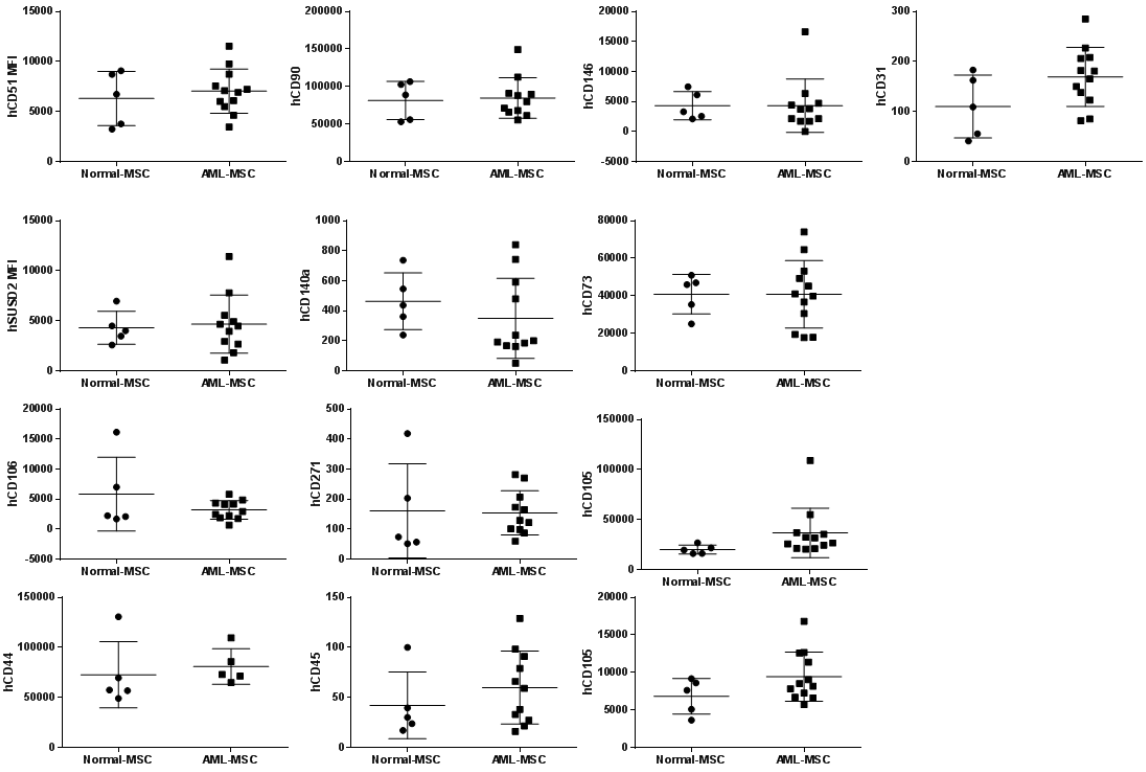

Supplementary Figure 4. *Cell surface expression of MSC associated markers in AML- and Normal-MSCs* . N-MSCs and AML-MSCs were immunophenotyped for indicated cell surface markers by flow cytometry. Mean florescence intensity (MFI) for each marker was generated by analyzing the data on FlowJo software. Graphs were generated using Prism software.

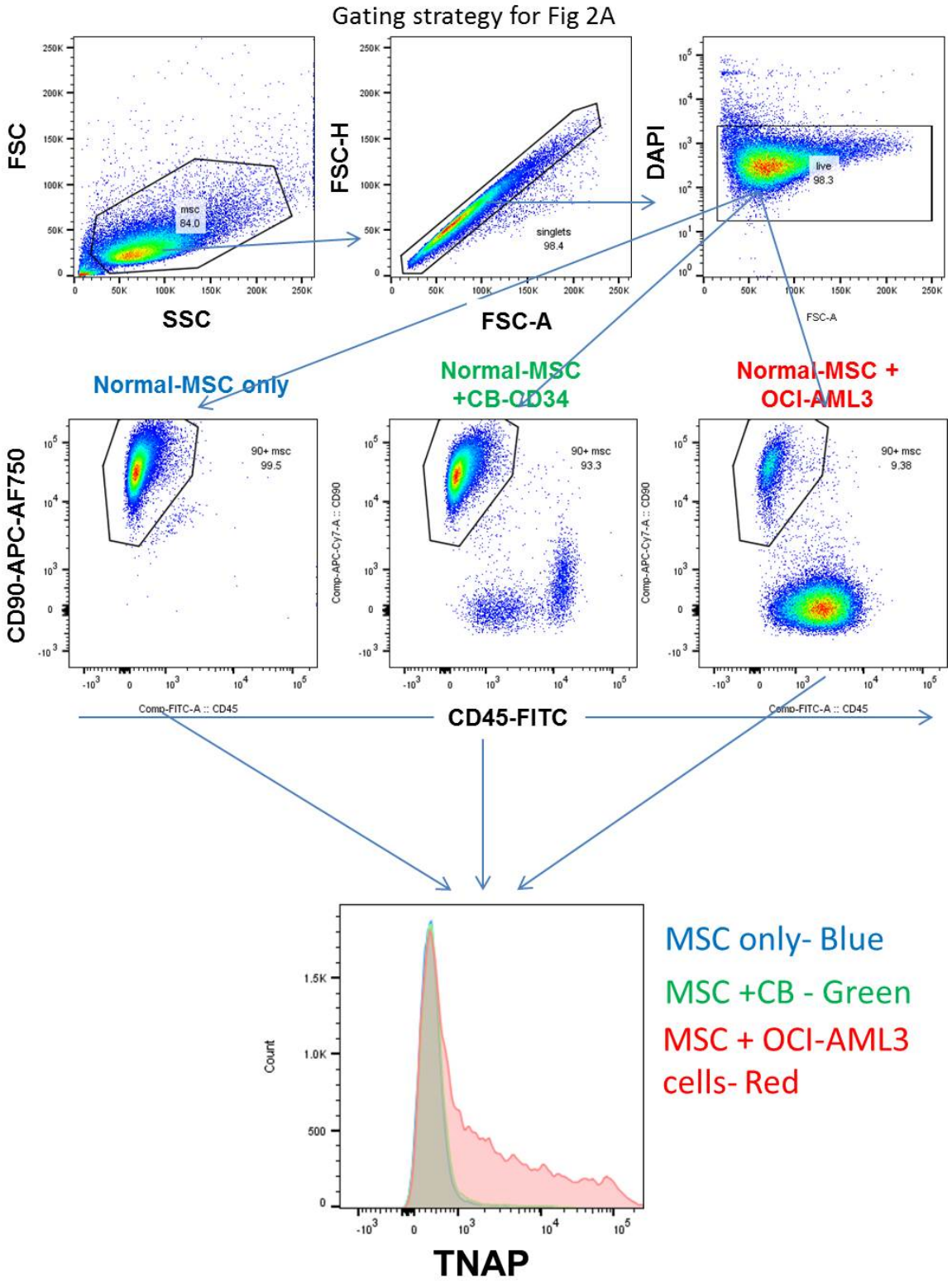

Supplementary Figure 5. *Gating strategy to examine TNAP expression on Normal-MSCs with or without cord blood (CB) derived CD34^{+} cells or OCI-AML3 cells.* N-MSCs were co-cultured

with OCI-AML3 cells or with CB-$CD34^+$ cells or Normal-MSCs cultured alone for 3 or 5 or 7 days. After incubation, the cells were tripsinized and incubated with anti-human CD90 conjugated with APC-Alexa flour-750 and anti-human CD45 conjugated with FITC and anti-human TNAP conjugated with-PE. Cells were initially gated on dual scatter dot plot and live cells were gated based on DAPI negative staining on LSR-II flow cytometer. The MSCs were gated as per their phenotype $CD90^+CD45^-$. TNAP expression on MSCs cultured with or without CB-$CD34^+$ or OCI-AML3 cells was analyzed by overlaying histograms generated by FlowJo software.

A)

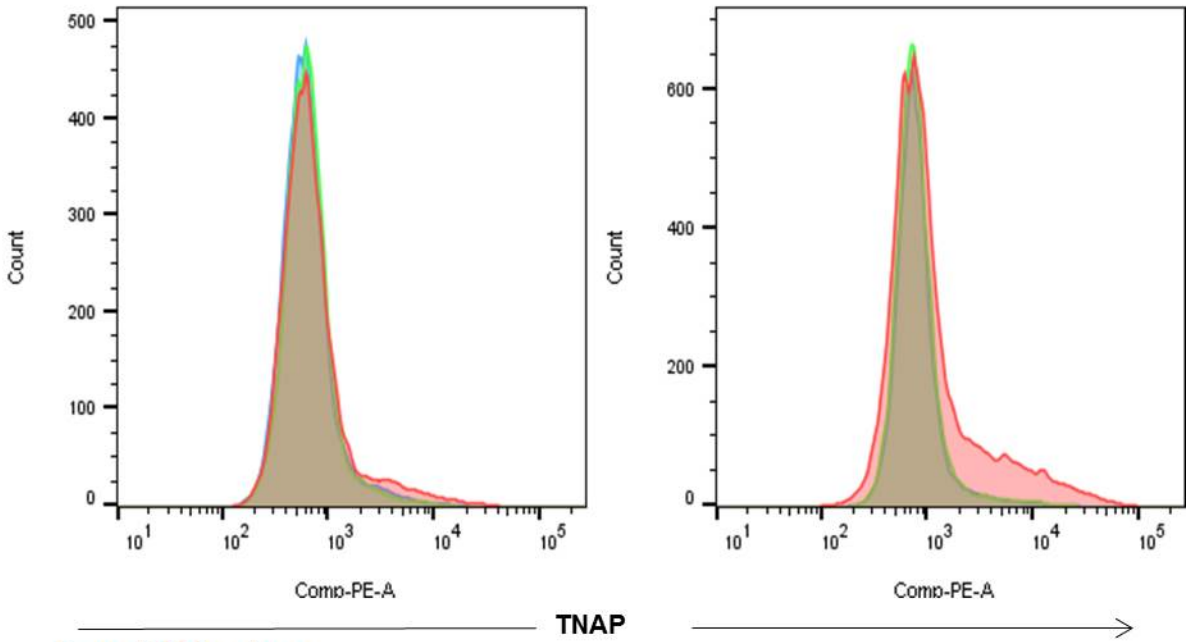
Count
Comp-PE-A
TNAP
Normal-MSCs alone
Normal-MSCs + Cord blood-CD33+ cells
Normal-MSCs + OCI-AML3 cells

B)

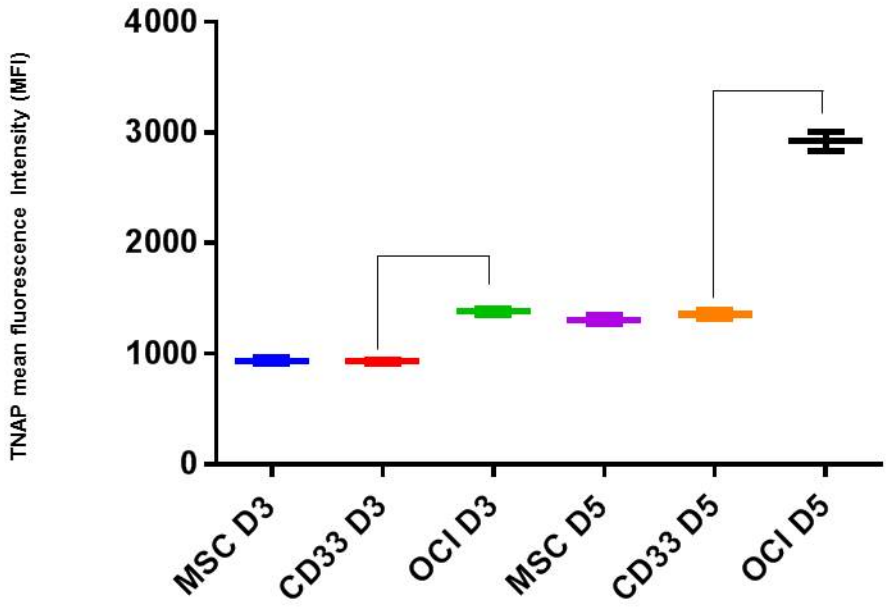
TNAP mean fluorescence Intensity (MFI)
MSC D3
CD33 D3
OCI D3
MSC D5
CD33 D5
OCI D5

Supplementary Figure 6. *AML cells induce osteogenic differentiation in N-MSCs.* (a) N-MSCs were co-cultured with OCI-AML3 cells(red) or with cord blood derived $CD33^+$ cells (green) or Normal-MSCs cultured alone (blue) for 3 or 5 days, and TNAP expression was analyzed by LSR-II flow cytometer (n=3). Data were analyzed and histograms generated by FlowJo software. (b) MFI of TNAP expression were quantified in N-MSCs monocultured or co-cultured with CB-$CD33^+$ or OCI-AML3 cells for 3 or 5 days.

A)

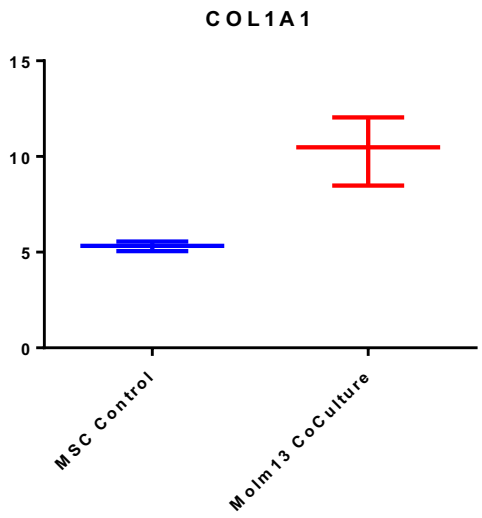
COL1A1
15
10
5
0
MSC Control
Molm13 CoCulture

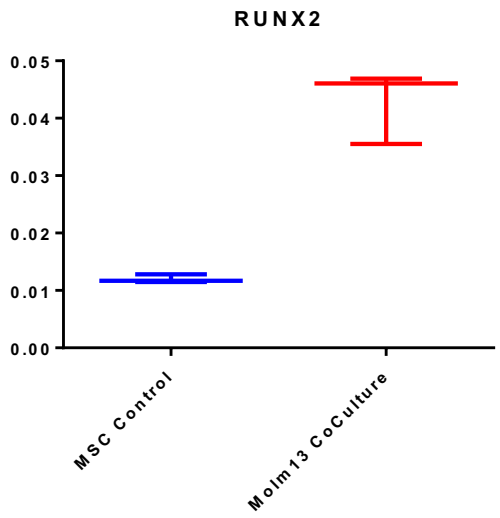
RUNX2
0.05
0.04
0.03
0.02
0.01
0.00
MSC Control
Molm13 CoCulture

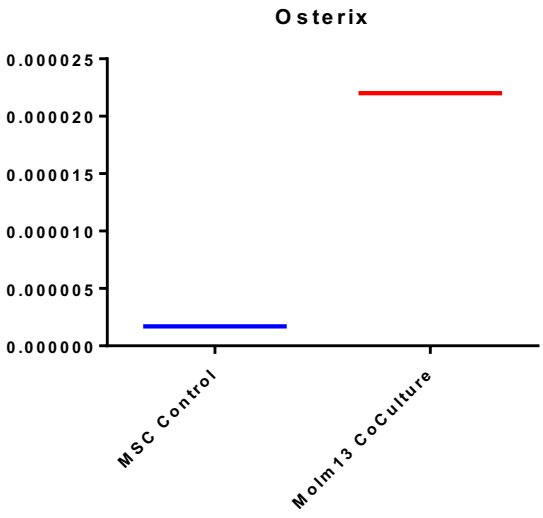
Osterix
0.000025
0.000020
0.000015
0.000010
0.000005
0.000000
MSC Control
Molm13 CoCulture

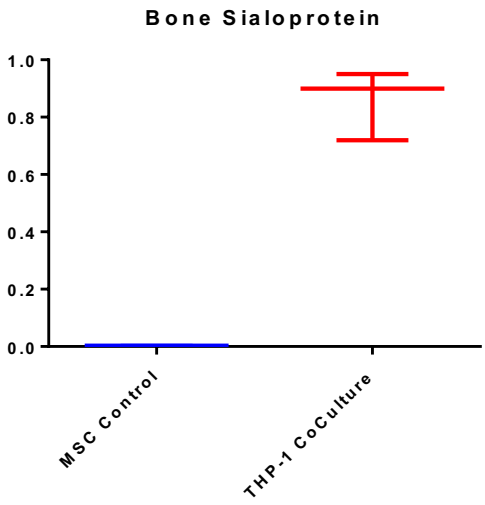
Bone Sialoprotein
1.0
0.8
0.6
0.4
0.2
0.0
MSC Control
THP-1 CoCulture

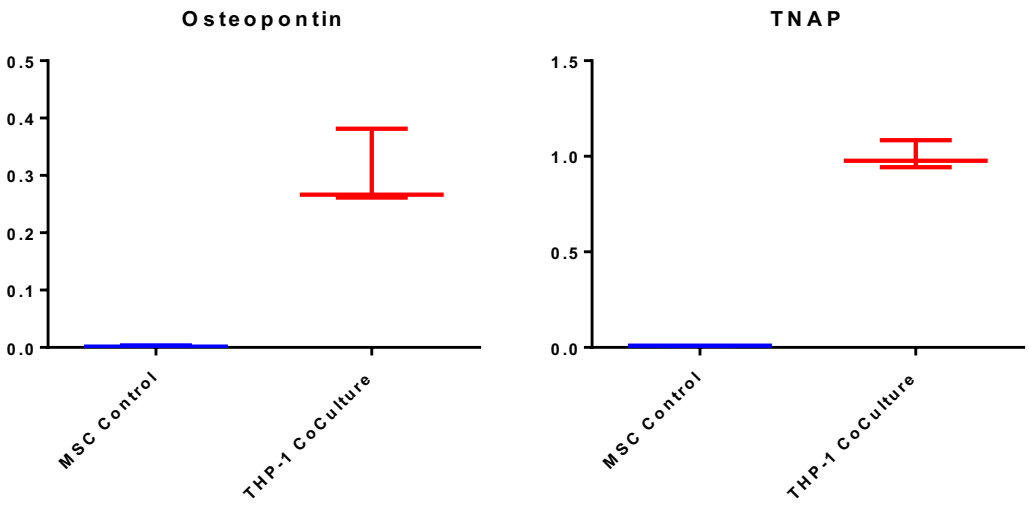
Osteopontin
0.5
0.4
0.3
0.2
0.1
0.0
MSC Control
THP-1 CoCulture
TNAP
1.5
1.0
0.5
0.0
MSC Control
THP-1 CoCulture

B)

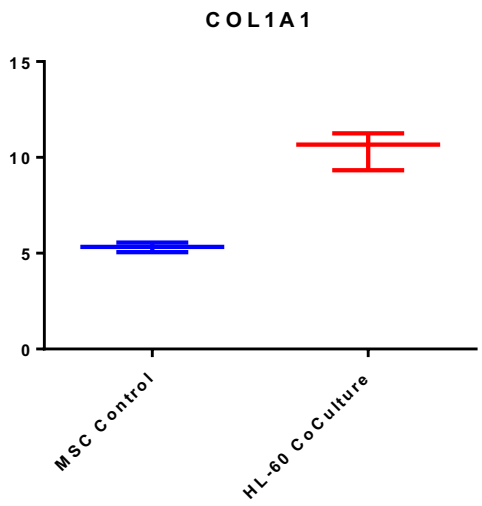
COL1A1
15
10
5
0
MSC Control
HL-60 CoCulture

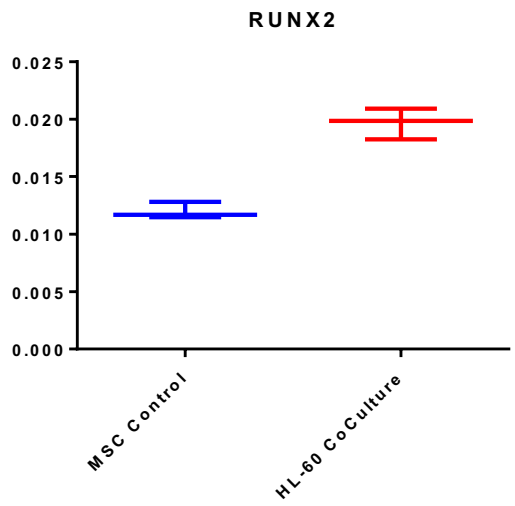
RUNX2
0.025
0.020
0.015
0.010
0.005
0.000
MSC Control
HL-60 CoCulture

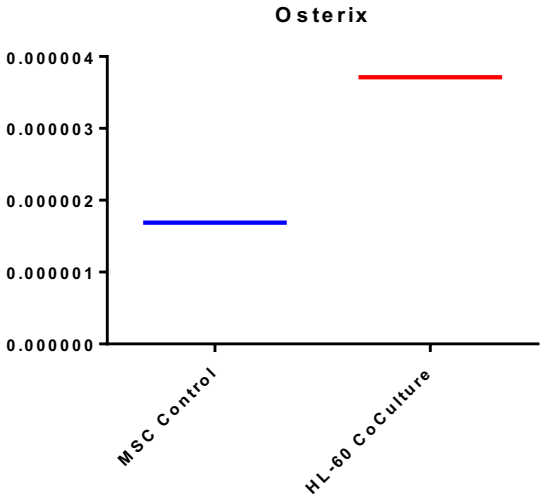
Osterix
0.000004
0.000003
0.000002
0.000001
0.000000
MSC Control
HL-60 CoCulture

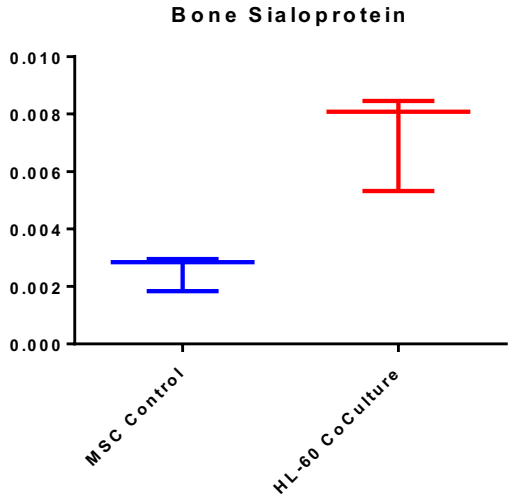
Bone Sialoprotein
0.010
0.008
0.006
0.004
0.002
0.000
MSC Control
HL-60 CoCulture

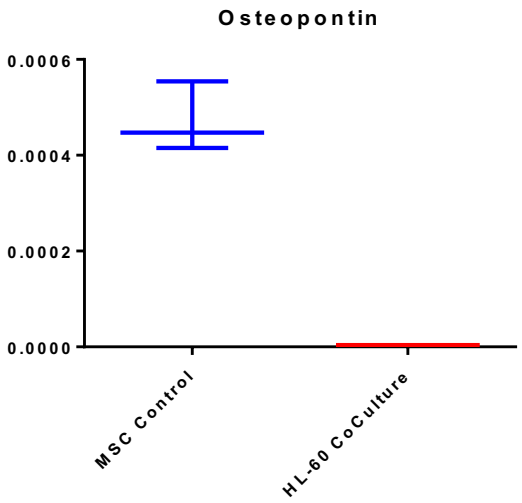
Osteopontin
0.0006
0.0004
0.0002
0.0000
MSC Control
HL-60 CoCulture

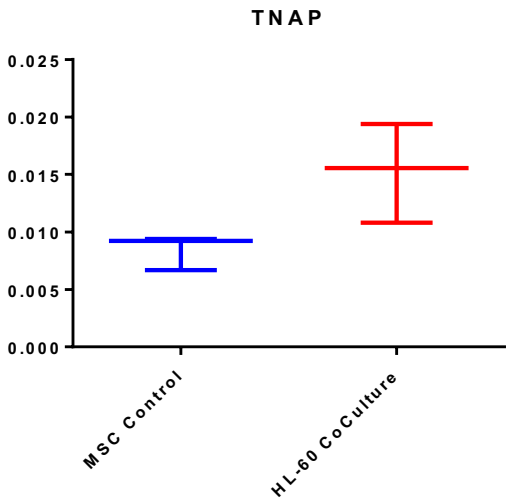
TNAP
0.025
0.020
0.015
0.010
0.005
0.000
MSC Control
HL-60 CoCulture

Supplementary figure 7: *AML cells induce osteogenic differentiation in N-MSCs.* AML cell lines including Molm13 (A) and HL60 (B) cells were co-cultured with or without N-MSCs for 5 days and MSCs were FACS sorted as described before. mRNA expression of osteogenic differentiation associated genes including col1a1, RUNX2, osterix, bone sialoprotein, osteopontin and TNAP in MSCs was measured by qRT-PCR. Relative gene expression to beta-actin is represented in bar graph.

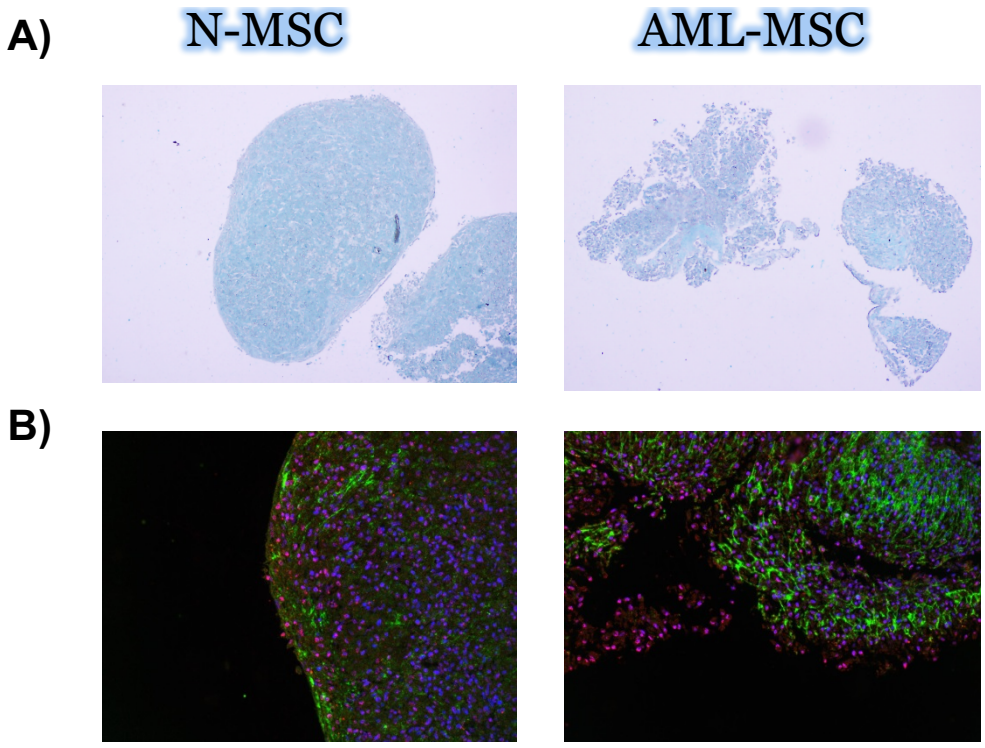

Supplementary Figure 8. *Chondrogenic differentiation is moderately affected in AML-MSCs.* After culture in chondrogenic differentiation medium for 28 days, N-MSCs and ALM-MSCs were subjected to (a) Alcian Blue staining or (b) immunostaining for collagen type-1 (green) or type-2 (red). The Opal multiplex staining method was used to develop the signal from antibody staining. Images were taken by using the Vectra multispectral imaging system.

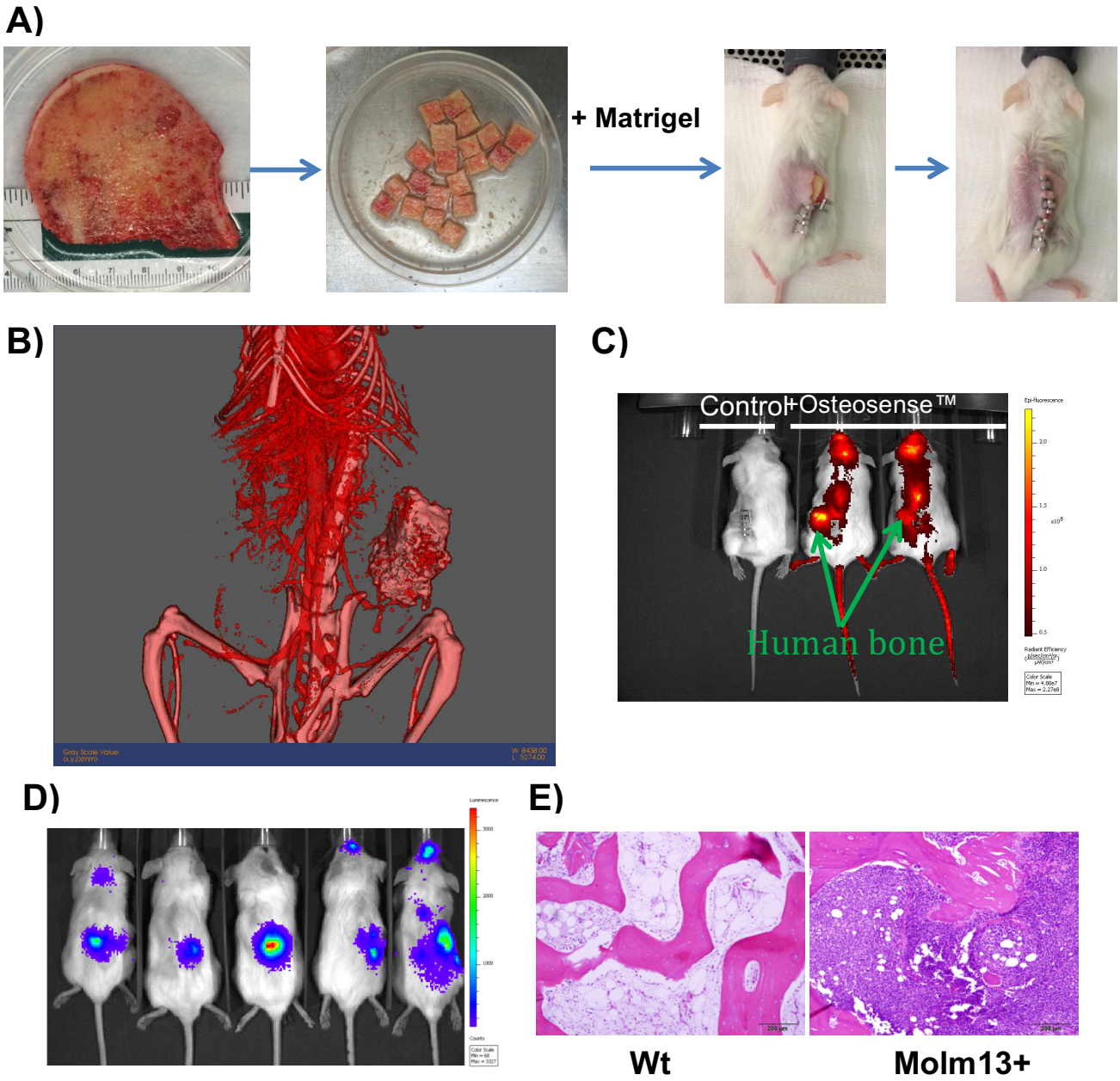

Supplementary Figure 9. *AML-induced osteogenic differentiation of MSCs is validated in the HBMI mouse model.* (a) Fragments of human femur were implanted into the flanks of NSG mice to model human bone marrow conditions. Fresh human femurs were cut into 1×1-cm pieces and mixed with matrigel. Two 1-cm incisions were made in the right flank of each mouse using a sterile sharp scalpel, and a human bone fragment was implanted subcutaneously into each

mouse. Surgical clips were used to fix the bone temporarily. (b) This video clip shows a CT scan of a representative HBMI mouse 4 weeks after bone fragment implantation. AuroVist 15 nm was used as the contrast agent to visualize the mouse vasculature. (c) HBMI mice and controls were injected intravenously with OsteoSense 750EX dye (100 ❣ L/mouse). The IVIS imaging system was used to visualize active bone generation, and the data were analyzed by Living Image software. (d) HBMI mice were injected intravenously with Molm13 AML cells (1×10^6) expressing firefly luciferase 4 weeks after bone fragment implantation (n=5). IVIS bioluminescence imaging was performed on day 10 after Molm13 cell transplantation. (e) H&E staining of representative human bone samples from HBMI mice transplanted with (right) or not transplanted with (left) Molm13 cells. Scale bar, 200 μm.

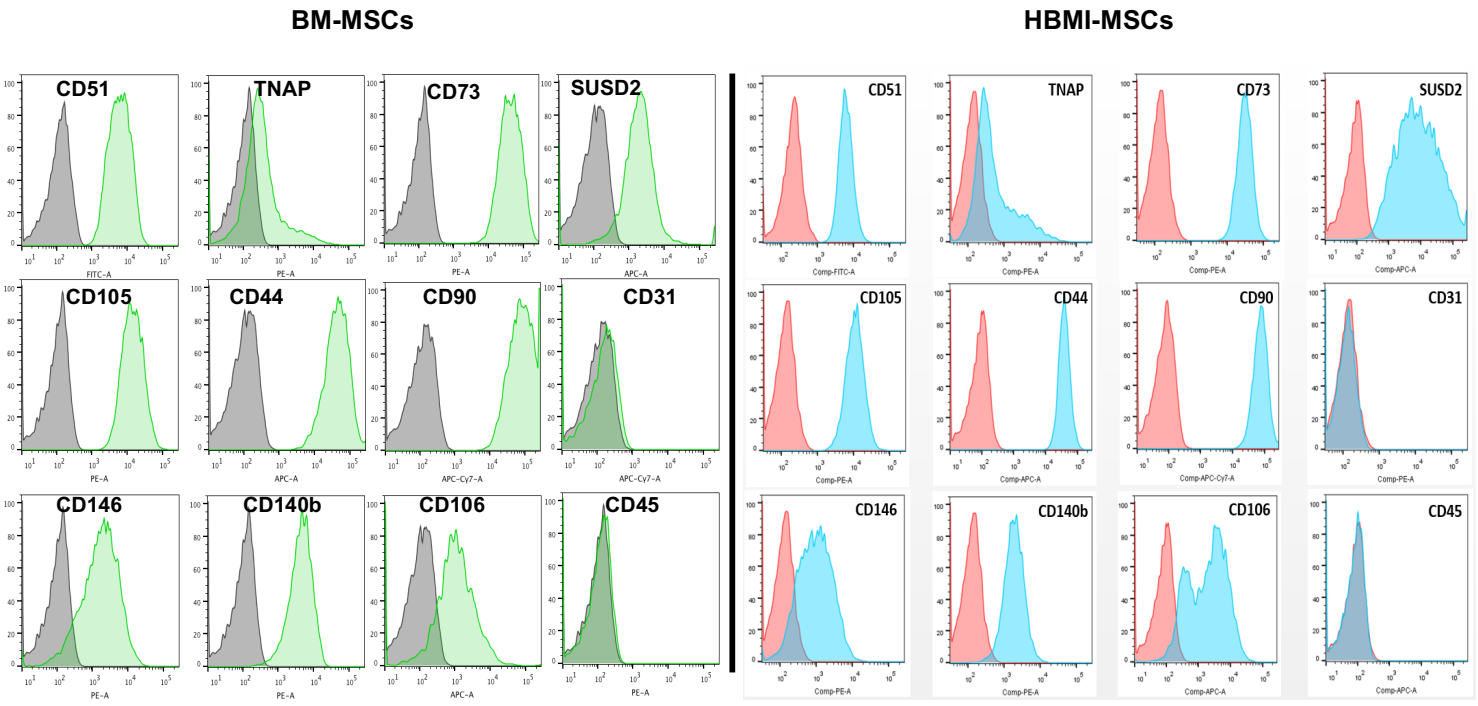

Supplementary Figure 10. *HBMI-derived MSCs are phenotypically and functionally similar to human BM-derived MSCs*. MSCs were extracted from HBMI mice and subjected to FACS using human CD140b and human CD90 antibodies. BM-MSCs (left) and HBMI-derived human MSCs

(right) were subjected to immunophenotyping analysis for selected MSC surface markers by flow cytometry. Data were analyzed by FlowJo software.

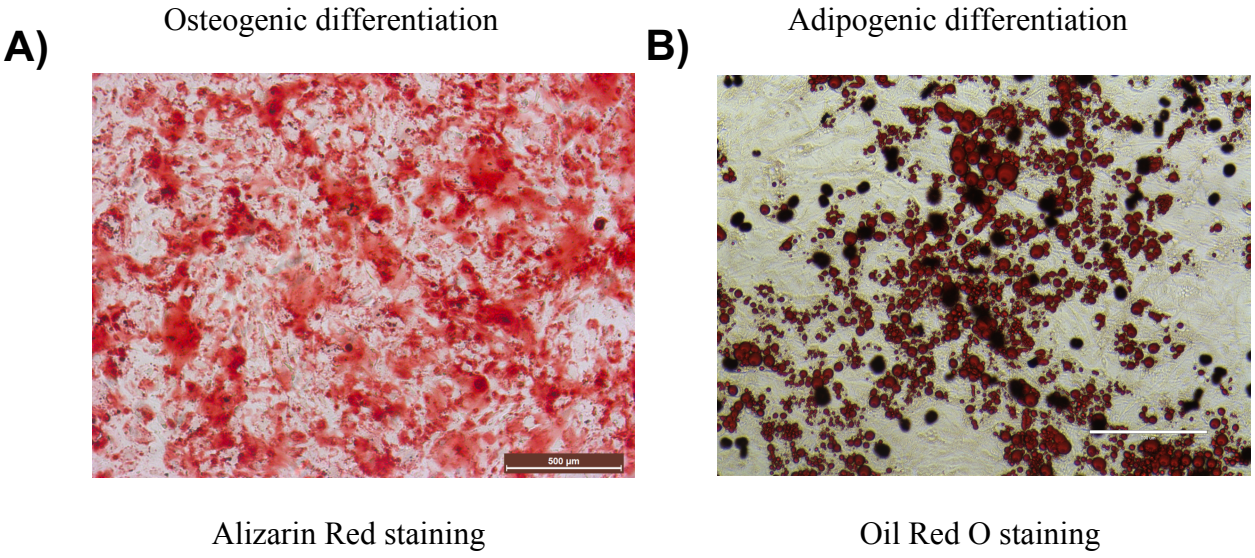

Supplementary Figure 11. *HBMI-derived MSCs differentiate into osteogenic and adipogenic lineage*. MSCs were extracted from HBMI derived from mice and subjected to osteogenic and adipogenic differentiation. (a) Alizarine Red S staining representing mineral deposition and mature osteoblast formation. (b) Oil Red O staining represents mature oil droplet formation and adipocyte differentiation of HBMI–derived MSCs.

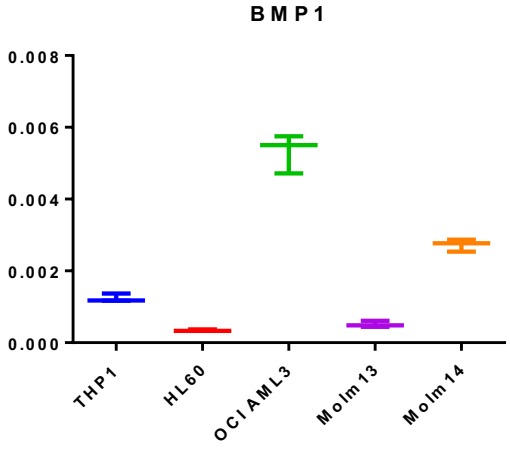
BMP1
0.008
0.006
0.004
0.002
0.000
THP1
HL60
OCIAML3
Molm13
Molm14

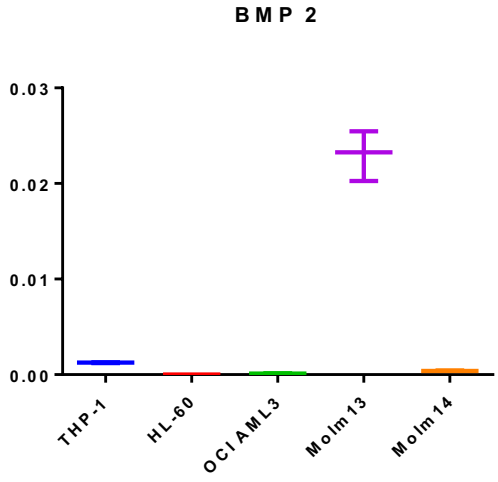
BMP 2
0.03
0.02
0.01
0.00
THP-1
HL-60
OCIAML3
Molm13
Molm14

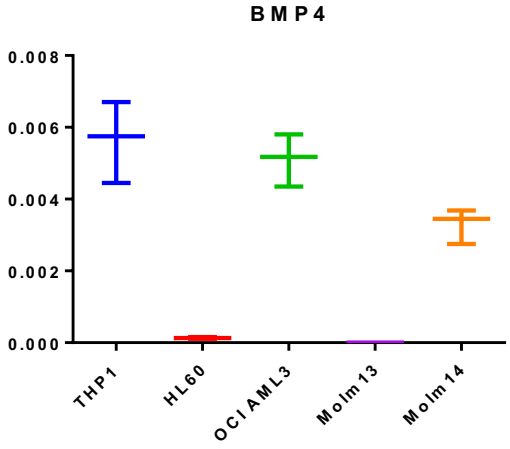
BMP4
0.008
0.006
0.004
0.002
0.000
THP1
HL60
OCIAML3
Molm13
Molm14

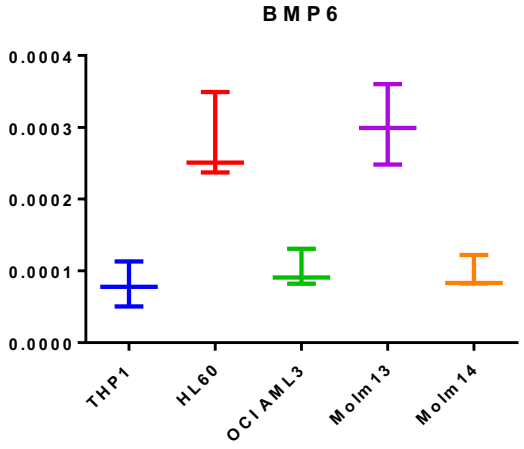
BMP6
0.0004
0.0003
0.0002
0.0001
0.0000
THP1
HL60
OCIAML3
Molm13
Molm14

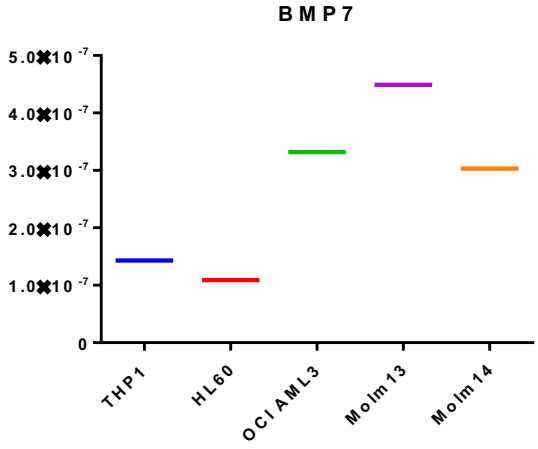
BMP7
5.0✖10 -7
4.0✖10 -7
3.0✖10 -7
2.0✖10 -7
1.0✖10 -7
0
THP1
HL60
OCIAML3
Molm13
Molm14

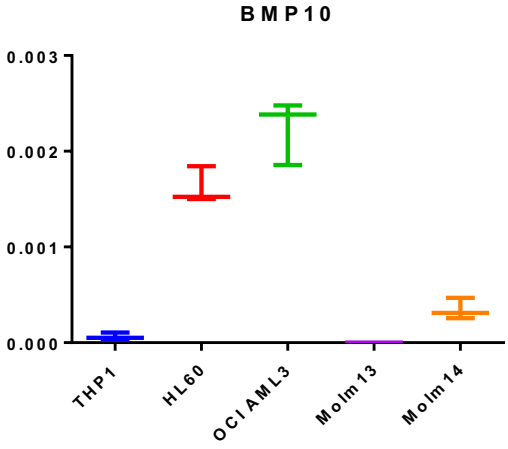
BMP10
0.003
0.002
0.001
0.000
THP1
HL60
OCIAML3
Molm13
Molm14

Supplementary Figure 12: BMP ligands expression in AML cell lines. mRNA from AML cell lines including Tnp1, HL60, OCI-AML3, molm13 and molm14 was isolated expression of BMP1, 2, 4, 6, 7, and 10 was analyzed by qRT-PCR. Relative expression of BMPs to beta-actin in AML cell lines is represented in bar graph.